Spin filtering and magnetoresistance in ballistic tunnel junctions

J. C. Egues*
Departamento de Física e Informática, Instituto de Física de São Carlos, Universidade de São Paulo, 13560-970 São Carlos, São Paulo, Brazil

C. Gould, G. Richter, and L. W. Molenkamp
Physikalisches Institut, Universität Würzburg, Am Hubland, 97074 Würzburg, Germany

(Received 15 March 2001; revised manuscript received 11 June 2001; published 19 October 2001)

We theoretically investigate magnetoresistance (MR) effects in connection with spin filtering in quantum-coherent transport through tunnel junctions based on nonmagnetic/semimagnetic heterostructures. We find that spin filtering in conjunction with the suppression/enhancement of the spin-dependent Fermi seas in semimagnetic contacts gives rise to (i) spin-split kinks in the MR of single barriers and (ii) a robust beating pattern in the MR of double barriers with a semimagnetic well. We believe these are unique signatures for quantum filtering.

DOI: 10.1103/PhysRevB.64.195319 PACS number(s): 72.25.Dc, 72.25.Hg, 73.23.Ad, 75.50.Pp

I. INTRODUCTION

The recent experimental demonstrations of spin-polarized currents in Mn-based semiconductors[1–3] represent a crucial first step towards understanding spin-dependent transport in these systems and possibly devising real spintronic devices.[4] So far spin injection has been verified only at cryogenic temperatures. Low temperature spin transport is, however, extremely important as a testing ground for novel ideas and concepts in the emerging fields of *semiconductor* spintronics and (possibly) quantum computing.[5]

The spin-injection experiments involving a semimagnetic layer as a spin aligner[6] reported to date[1–3] pertain to transport in the *diffusive* limit. Moreover, the high voltages used ($eV \gg$ Fermi energy) make transport highly *nonlinear*. More recently, Schmidt *et al.*[7] have investigated MR in diffusive spin transport through a nonmagnetic semiconductor (NMS) layer with dilute-magnetic semiconductor (DMS) contacts. In the regime of linear response they find a positive MR due to the suppression of one spin channel in the nonmagnetic region.

The ballistic or quantum-coherent limit is another interesting regime in which to look at spin-polarized transport. In this regime, *spin filtering*[8] can give rise to a spin-polarized flow. As detailed in Ref. 8, spin filtering in semimagnetic systems is due to selective electron transmission. The s-d interaction gives rise to a spin-dependent potential: spin-up and spin-down electrons see different barrier heights. Hence one spin component is blocked while the other is not. Observe that in diffusive transport *spin aligning*[6] due to spin-flip processes is the dominant mechanism behind the generation of spin-polarized currents in semimagnetic semiconductors.

Here we theoretically investigate MR for ballistic transport in semimagnetic heterojunctions[9] with several arrangements of semimagnetic contacts and tunnel barriers as shown in Figs. 1(a)–1(h). The idea is to find signatures of the spin-filtering effect in the MR; so far no experimental evidence for spin filtering in semimagnetic heterostructures has been reported. Our current density calculation follows that of Ref. 8 properly generalized to account for *spin-dependent contacts*. We calculate the spin-up and spin-down linear[10] con-

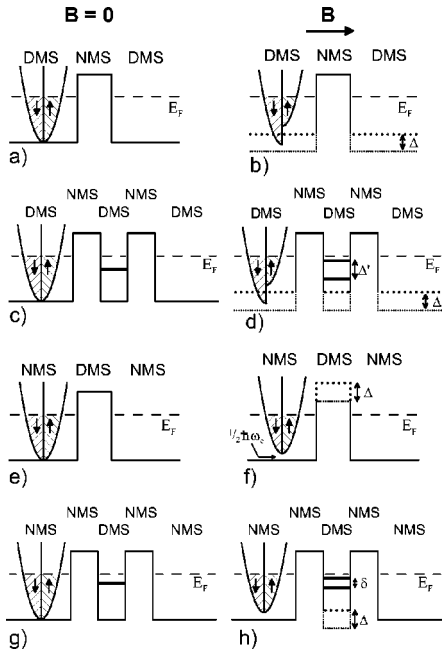

FIG. 1. Spin-dependent potential profiles for several tunneling structures. In DMS-contacted geometries with applied B, the s-d exchange interaction shifts the spin-up and spin-down band edges upwards and downwards, respectively, relative to the $B=0$ case, thus creating partially spin-polarized reservoirs [only subbands for the lowest Landau levels are shown: $\hbar\omega_c/2 \pm \epsilon(B) + \hbar^2 k_z^2/2m_e^*$]. This is illustrated in (a) and (b) for a single barrier and in (c) and (d) for a double barrier. A single DMS barrier with NMS contacts is shown in (e) and (f). Note that now the s-d interaction modulates only the barrier height in a spin-dependent fashion; the electron reservoirs are here unpolarized. The NMS-contacted double-barrier structure with a DMS well is shown in (g) and (h). The left panel shows only the lowest Landau level bands (contacts) for $B \neq 0$. A particularly large spin splitting is attained by using a DMS-contacted double-barrier geometry with semimagnetic well in contrast to the nonmagnetic contact case: $\Delta' - \delta \approx \Delta = 2\epsilon(B)$.

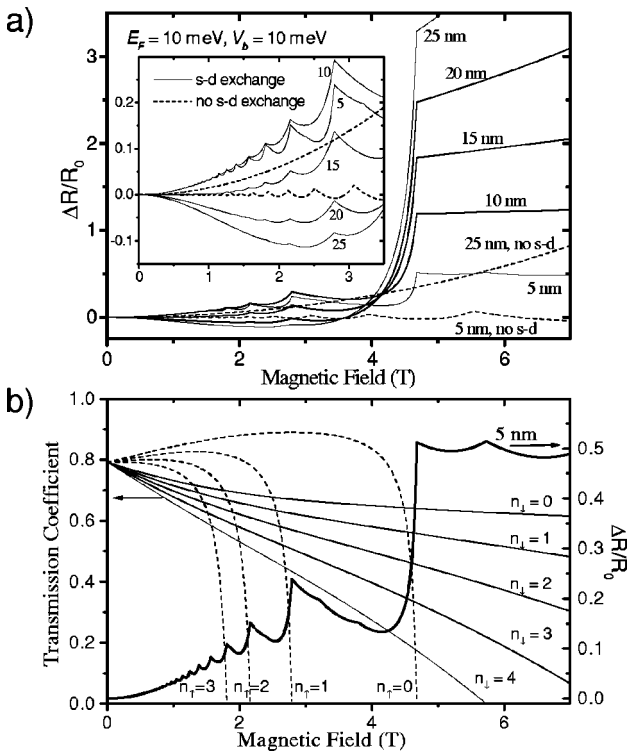

FIG. 2. Magnetic-field dependence of $\Delta R/R_0$ (a) and transmission coefficients (b) for single NMS barriers with DMS contacts, Fig. 1(a). Exchange-induced filtering in conjunction with the corresponding reduction of the spin-up phase space below E_F in the DMS contacts gives rise to an enhanced positive MR for larger barrier widths as compared to the no s-d case (dashed lines). The MR is slightly negative for small fields and larger barriers (inset). The usual kinks due to Landau-level quantization are also present; however, they are now more pronounced and spin resolved (b). We can also see the kinks are due to the subsequent shut down of spin-resolved transmission channels as the field is increased. Note that current should be fully spin polarized for $B>4.7$ T.

ductances in terms of the respective transmission coefficients and present explicit formulas for single- and double-barrier cases.

Findings. For single-barrier structures with DMS contacts and NMS barriers, Figs. 1(a) and 1(b), we find that spin filtering and the spin-dependent changes of the Fermi seas in the contacts give rise to an enhanced and essentially positive MR, Fig. 2(a). Spin-split kinks in MR are also seen, Fig. 2(b); these result from subsequent spin-resolved Landau levels crossing the Fermi surface in the contacts and hence closing the corresponding conducting channels. For double-barrier systems comprised of DMS contacts and well with nonmagnetic barriers, Figs. 1(c) and 1(d), we find particularly interesting beating in the MR. This robust feature comes about because of the *significantly enhanced* spin splitting of the resonant levels in the well; this results from the unique alignment of spin-dependent band edges in the contacts with the respective bottom of the potential well—provided by the particular geometry used. For semimagnetic barriers with nonmagnetic contacts, Figs. 1(e) and 1(f), spin filtering suppresses the Landau-level-induced kinks and makes MR essentially negative, Fig. 3.

The above features markedly contrast with the MR in nonmagnetic heterostructures. We believe the peculiar structures in the MR of semimagnetic heterojunctions constitute unique signatures of the interplay between quantum spin filtering and spin-dependent phase-space modulation in the contacts.

II. MODEL SYSTEM

Consider a two-terminal geometry with DMS contacts separated by a tunneling region. In the presence of a magnetic field B along the growth direction z, the transverse motion is quantized into Landau levels.[11] Along the field we have parabolic spin-dependent bands $\xi_{\sigma_z}(k_z,B)=\varepsilon_{\sigma_z}(B)+E_z(k_z)$ with $E_z(k_z)=\hbar^2k_z^2/2m_e^*$, k_z is the electron wave vector and m_e^* the effective mass. The spin-dependent band edges are $\varepsilon_{\sigma_z}\equiv\pm\epsilon(B)$, where the upper sign refers to spin-up electrons and $\epsilon(B)\equiv x_{\rm eff}|\langle S_z\rangle|N_0\alpha/2>0$, $x_{\rm eff}=x(1-x)$[12] is the effective Mn concentration (accounting for Mn-Mn antiferromagnetic pairing), $\langle S_z\rangle$ is the 5/2 Brillouin function describing the thermal average of the Mn spin components, and $N_0\alpha$ is the s-d exchange constant for conduction electrons.

Current density. The tunneling region is described by a spin-dependent transmission coefficient $T_{\sigma_z}(E_z,V,B)$. By extending the approach in Ref. 8 to the present case we can write the current density across the tunneling region at zero temperature[12] and for $eV<E_F$ as

$$J_{\sigma_z}(B)=\overline{J}_0\hbar\omega_c\Bigg\{\int_0^{E_F^{\sigma_z}-\frac{1}{2}\hbar\omega_c}\left[\mathrm{int}\left(\frac{E_F^{\sigma_z}-E_z}{\hbar\omega_c}-\frac{1}{2}\right)+1\right]\times T_{\sigma_z}(E_z,V,B)dE_z-\int_0^{E_F^{\sigma_z}-\frac{1}{2}\hbar\omega_c-eV}\times\left[\mathrm{int}\left(\frac{E_F^{\sigma_z}-eV-E_z}{\hbar\omega_c}-\frac{1}{2}\right)+1\right]\times T_{\sigma_z}(E_z,V,B)dE_z\Bigg\}, \tag{1}$$

where $\overline{J}_0\equiv em_e^*/4\pi^2\hbar^3$, $E_F^{\uparrow,\downarrow}=E_F\mp\epsilon(B)$, ω_c is the cyclotron frequency, and $\mathrm{int}(x)$ denotes the largest integer smaller than or equal to x. Equation (1) is the $B\neq0$ Tsu-Esaki formula with spin-dependent transmission coefficients.

A. Linear Response

Linear spin-dependent conductance. To determine the linear conductance we linearize Eq. (1). Taylor expanding Eq. (1) around $eV=0$ and using

$$\frac{d\,\mathrm{int}(x)}{deV}=\frac{d\,\mathrm{int}(x)}{dx}\frac{\partial x}{\partial eV}=-\frac{1}{\hbar\omega_c}\sum_n\delta(x-n), \tag{2}$$

where n is an integer and $x=(E_F^{\sigma_z}-eV-E_z)/\hbar\omega_c-\frac{1}{2}$, we find to linear order in eV

$$J_{\sigma_z}(B,E_F,eV)=\overline{J}_0\hbar\omega_c\sum_{n=0}^{n_0^{\sigma_z}} T_{\sigma_z}(E_{F,n}^{\sigma_z},0,B)eV, \qquad (3)$$

with $n_0^{\sigma_z}=\mathrm{int}(E_F^{\sigma_z}/\hbar\omega_c-\frac{1}{2})$ and $E_{F,n}^{\sigma_z}\equiv E_F^{\sigma_z}-(n+\frac{1}{2})\hbar\omega_c$. The spin-dependent linear conductance per unit area $G_{\sigma_z}(B,E_F)/A\equiv J_{\sigma_z}(B,E_F,V)/V$ is

$$G_{\sigma_z}(B,E_F)/A=\frac{e^2m_e^*}{4\pi^2\hbar^3}\hbar\omega_c\sum_{n=0}^{n_0^{\sigma_z}} T_{\sigma_z}(E_{F,n}^{\sigma_z},0,B). \qquad (4)$$

Observe that the transmission coefficient in Eq. (4) is calculated *in the absence* of any external potential; this is just the general philosophy of linear response: the response depends upon only the system configuration in equilibrium. It is straightforward to verify that Eq. (4) reduces to the well known result[13]

$$G_0(E_F)/A=\frac{e^2m_e^*}{4\pi^2\hbar^3}\int_0^{E_F} dE_z T_0(E_z), \qquad (5)$$

in the $B=0$ limit, where $G_0(E_F)\equiv G_\uparrow(E_F,0)=G_\downarrow(E_F,0)$ and $T_0(E_z)\equiv T_\uparrow(E_z,0)=T_\downarrow(E_z,0)$.

B. Magnetoresistance

Let R (R_0) and G ($\tilde{G}_0=2G_0$) be the *total* resistance and conductance, respectively, in the presence (absence) of magnetic fields. The MR of the system is defined by $\Delta R/R_0=R/R_0-1=\tilde{G}_0/G-1=2G_0(E_F)/[G_\uparrow(B,E_F)+G_\downarrow(B,E_F)]-1$. Hence

$$\frac{\Delta R}{R_0}=\frac{2\int_0^{E_F} dE_z T_0(E_z)}{\hbar\omega_c\left[\sum_{n=0}^{n_0^\uparrow} T_\uparrow(E_{F,n}^\uparrow,B)+\sum_{n=0}^{n_0^\downarrow} T_\downarrow(E_{F,n}^\downarrow,B)\right]}-1. \qquad (6)$$

In deriving Eq. (6) we assume a negligible contact resistance.

C. Transmission Coefficients

Single- and double-barrier potentials. In order to determine $\Delta R/R_0$ from Eq. (6) we only need the transmission coefficients for *zero* applied voltage (equilibrium configuration) since we are in the linear response regime. For a single barrier of width L_b and height V_b we readily find[8]

$$T_{\uparrow,\downarrow}^{SB}(E_{F,n}^{\uparrow,\downarrow},B)=\left\{1+\frac{\sinh^2\left[\sqrt{\frac{2m_e^*(V_{\uparrow,\downarrow}-E_{F,n}^{\uparrow,\downarrow})}{\hbar^2}}L_b\right]}{4\left(\frac{E_{F,n}^{\uparrow,\downarrow}}{V_{\uparrow,\downarrow}}\right)\left(1-\frac{E_{F,n}^{\uparrow,\downarrow}}{V_{\uparrow,\downarrow}}\right)}\right\}^{-1}, \qquad (7)$$

with $V_{\uparrow,\downarrow}=V_b\mp\epsilon(B)$ and $E_{F,n}^{\uparrow,\downarrow}=E_F\mp\epsilon(B)-(n+1/2)\hbar\omega_c$.

For a symmetric DMS-contacted double-barrier structure with a semimagnetic well of width L_w and NMS barriers of width L_b and height V_b, we have

$$T_{\uparrow,\downarrow}^{DB}(E_{F,n}^{\uparrow,\downarrow},B)=\left|\left[\cosh(\kappa_n^{\uparrow,\downarrow}L_b)-i\frac{2E_{F,n}^{\uparrow,\downarrow}-V_{\uparrow,\downarrow}}{2\sqrt{E_{F,n}^{\uparrow,\downarrow}(V_{\uparrow,\downarrow}-E_{F,n}^{\uparrow,\downarrow})}}\sinh(\kappa_n^{\uparrow,\downarrow}L_b)\right]^2 e^{-ik_n^{\uparrow,\downarrow}L_w}\right.$$
$$\left.+\frac{V_{\uparrow,\downarrow}^2}{4E_{F,n}^{\uparrow,\downarrow}(V_{\uparrow,\downarrow}-E_{F,n}^{\uparrow,\downarrow})}\sinh^2(\kappa_n^{\uparrow,\downarrow}L_b)e^{ik_n^{\uparrow,\downarrow}L_w}\right|^{-2}, \qquad (8)$$

where $k_n^{\uparrow,\downarrow}=\sqrt{2m_e^*E_{F,n}^{\uparrow,\downarrow}}/\hbar$ and $\kappa_n^{\uparrow,\downarrow}=\sqrt{2m_e^*(V_{\uparrow,\downarrow}-E_{F,n}^{\uparrow,\downarrow})}/\hbar$. Equations (7) and (8) hold for $V_{\uparrow,\downarrow}\geq E_{F,n}^{\uparrow,\downarrow}$. In what follows we discuss some plots of $\Delta R/R_0$ vs B for both single- and double-barrier heterostructures. In the subsequent graphs we use $x=0.06$ and $m_e^*=0.16m_0$. Fermi energies and potential heights (and widths) are shown in the figures.

III. RESULTS

Results. Figure 2 shows the MR of a DMS/NMS/DMS structure, Figs. 1(a) and 1(b), for several NMS barrier widths. Observe that the MR is *enhanced and mostly positive* for wider barriers and high fields, as compared to the nonmagnetic case (dashed lines). These features are due to spin

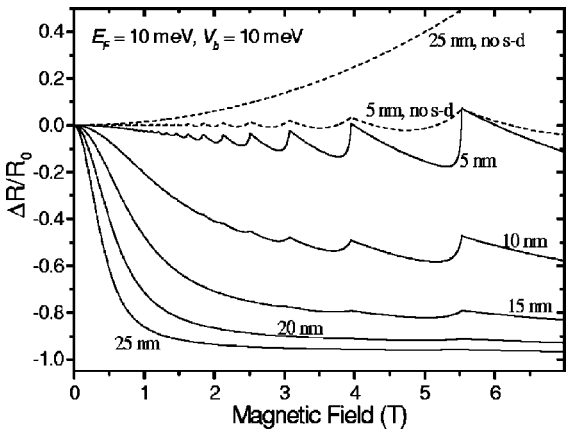

FIG. 3. Same as Fig. 2(a) but for a NMS/DMS/NMS structure [see Fig. 1(e)]. Much in contrast to the DMS-contacted barrier case in Fig. 2(a) and the no s-d exchange case (dashed lines), spin filtering here gives rise to enhanced negative $\Delta R/R_0$ for wider barriers. Narrower DMS barriers show smaller MR and kinks similar to the no s-d case; however, the Landau levels here are not spin resolved.

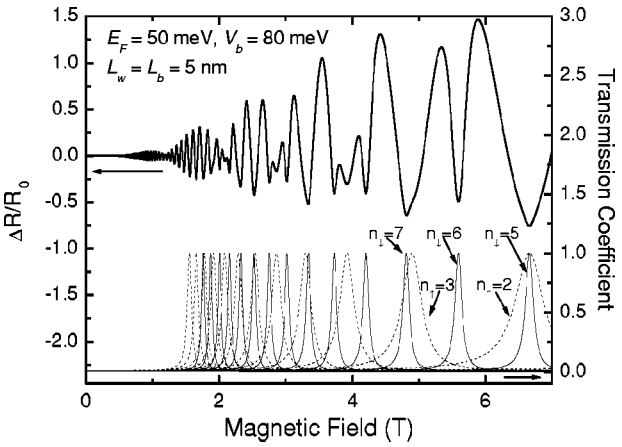

FIG. 4. Beating in the MR of a double-barrier system with both DMS well and contacts [see Fig. 1(c)]. The beating feature in the MR response is due to the overlap of many s-d spin-resolved transmission channels, as clearly shown in the lower part of the figure. The large spin splitting of the spin-resolved resonant level in the well—unique to a geometry in which, for each spin component, the corresponding bottom of the potential in the well is aligned with the respective conduction band edge in the contacts–makes this beating very pronounced; a strong signature of quantum-coherent spin-resolved transport in double barriers.

filtering resulting from the relative change of the band edges in the DMS contacts together with the concomitant reduction and increase of the Fermi seas for spin-up and spin-down electrons, respectively. Positive MR is expected for high enough fields above which the spin-up channels are unavailable. Here, for $B>4.7$ T the spin-up conductance is identically zero; see the kink and the steep rise of $\Delta R/R_0$ around $B=4.7$ T for all barrier widths. Note that because the conductance of the system is essentially a sum over spin-resolved Landau channels smaller than $n_0^{\uparrow,\downarrow}$, Eq. (4), the abrupt closing of channels manifests itself directly in $\Delta R/R_0$ via Eq. (6). Figure 2(b) illustrates the connection between the shut down of spin-resolved transmission channels and the kinks in the MR more clearly. Note that the more abruptly a channel shuts down, the steeper $\Delta R/R_0$ rises in its vicinity. Note also that the spin-resolved Landau levels give rise to spin-split kinks in the MR. The inset shows that the interplay between spin-dependent phase space in the DMS contacts and spin filtering can also lead to negative MR for larger barriers and smaller fields. All the above features contrast with the no s-d exchange case (dashed lines).

Figure 3 shows a plot similar to that in Fig. 2 but for a single DMS barrier with NMS contacts.[14] Note that the MR is now *mostly negative*. Here this happens entirely because of quantum-coherent spin filtering.[8] As the magnetic field increases the spin-up (spin-down) electrons see a larger (smaller) barrier. The corresponding exponential suppression of $T_\uparrow$ and the concomitant enhancement of $T_\downarrow$ is asymmetric. Because the wave function penetration in the DMS barrier is larger for spin down than for spin up electrons, the former see a stronger s-d modulation of the barrier height than the latter; $T_\downarrow$ then increases faster than $T_\uparrow$ decreases. Hence the total trasmission coefficient $T_\uparrow+T_\downarrow$ increases as compared to the $B=0$ case thus leading to $\Delta R/R_0<0$. This effect is more pronounced for larger barrier widths. For narrower barriers $\Delta R/R_0$ vs B also presents kinks and regions of positive and negative MR (see curves for the 5 and 10 nm barriers in Fig. 3).

Figure 4 shows our results for a symmetric DMS-contacted double-barrier system with a semimagnetic well and non-magnetic barriers. The $B=0$ configuration is chosen so that there is a resonant level below E_F for the parameters used. A remarkable feature in Fig. 4 is the beating in the MR.[15] As shown in the lower part of this figure, this beating is directly related to the peculiar overlap of the s-d spin-split transmission channels. The unique pattern in $\Delta R/R_0$ is made particularly noticeable by the geometry used—which effectively enhances s-d induced features. By considering semimagnetic contacts *and* well, we are essentially forcing the spin-resolved resonant states in the well to have larger spin splittings, Figs. 1(c) and 1(d). This happens because the spin-dependent bottom of the potential well lines up with the corresponding spin-split band edges in the DMS contacts. In simpler terms, we are referring the spin-resolved states to spin-split origins in the contacts. The end result is indeed a larger effective spin-splitting of the resonant levels. Note that the DMS contacts do not need to be fully spin polarized.

Feasibility. Recent advances in DMS materials technology make the short term realization of the structures suggested in this paper realistic.[16] For instance, combined DMS-NMS heterostructures have already been demonstrated[7] in ZnBeMnSe/ZnBeSe quartenary materials. The band offsets and doping densities achievable by varying the concentrations of these compounds are flexible enough to produce the potential profiles and Fermi energies considered here. Furthermore, we estimate the electron coherence lengths in these materials to be longer than the total length of our structures thus allowing for quantum-coherent transport.

Summary. We have shown that DMS-contacted tunnel junctions display very peculiar MR due to quantum-coherent spin filtering in conjunction with the reduction/enhancement of the spin-dependent Fermi seas in the contacts. The features in the MR reported here (e.g., beating and spin-split kinks) are unique signatures of spin filtering in ballistic transport. We expect these effects to be easily resolved experimentally.

ACKNOWLEDGMENTS

This work was supported by FAPESP and Deutsche Forschungsgemeinschaft (DFG, SFB 410). J.C.E. acknowledges the kind hospitality at the Physikalisches Institut, Universität Würzburg, where part of this work was developed, and financial support for his visit.

*Electronic address: egues@if.sc.usp.br

[1] R. Fiederling *et al.*, Nature (London) **402**, 787 (1999).
[2] Y. Ohno *et al.*, Nature (London) **402**, 790 (1999).
[3] B.T. Jonker *et al.*, Phys. Rev. B **62**, 8180 (2000).
[4] G. Prinz, Science **282**, 1660 (1998).
[5] G. Burkard *et al.*, Fortschr. Phys. **48**, 965 (2000).
[6] M. Oestreich *et al.*, Appl. Phys. Lett. **74**, 1251 (1999).
[7] G. Schmidt *et al.* (unpublished).
[8] J.C. Egues, Phys. Rev. Lett. **80**, 4578 (1998); see also Y. Guo *et al.*, Phys. Rev. B **55**, 9314 (1997), for transport in asymmetric multiple-barrier magnetic nanostructures (wave-vector filtering).
[9] Spin filtering and MR in the context of metallic multilayers is discussed by M.S. Ferreira *et al.*, J. Phys.: Condens. Matter **12**, L373 (2000); D.C. Worledge and T.H. Geballe, J. Appl. Phys. **88**, 5277 (2000); See also Wu-Shou Zhang *et al.*, Phys. Rev. B **58**, 14 959 (1998).
[10] K. Chang and F. M. Peeters (unpublished).
[11] We neglect Landau-level broadening; it is assumed much smaller than the relevant s-d energy splitting.
[12] As usual, we consider the electrons at $T=0$ (sharp Fermi function) and the paramagnetic impurities at $T=4.0$ K.
[13] See, for instance, C. B. Duke, *Tunneling in Solids*, supplement to Solid State Physics (Academic, New York, 1960), Vol. 10, Chap. IV, p. 60.
[14] The formulas for the conductances, magnetoresistance, and transmission coefficients for NMS-contacted structures are similar to those for the DMS-contacted ones. But now $n_0^{\uparrow}=n_0^{\downarrow}=n_0 \equiv \mathrm{int}(E_F/\hbar\omega_c-1/2), E_F^{\uparrow,\downarrow}=E_{F,n}\equiv E_F-(n+1/2)-\hbar\omega_c$, and $V_{\uparrow,\downarrow}=V_b\pm\epsilon(B)$ (i.e., "$\mp$" in the former definition of $V_{\uparrow,\downarrow}$ becomes "$\pm$" here).
[15] See J.J. Baumberg *et al.*, Phys. Rev. Lett. **72**, 717 (1994) for beating in magneto-optics.
[16] Detrimental effects (e.g., electron-electron interaction, band bending, etc.) and possible ways to minimize them are discussed in the paragraph *"Important points"* in Ref. 8.